

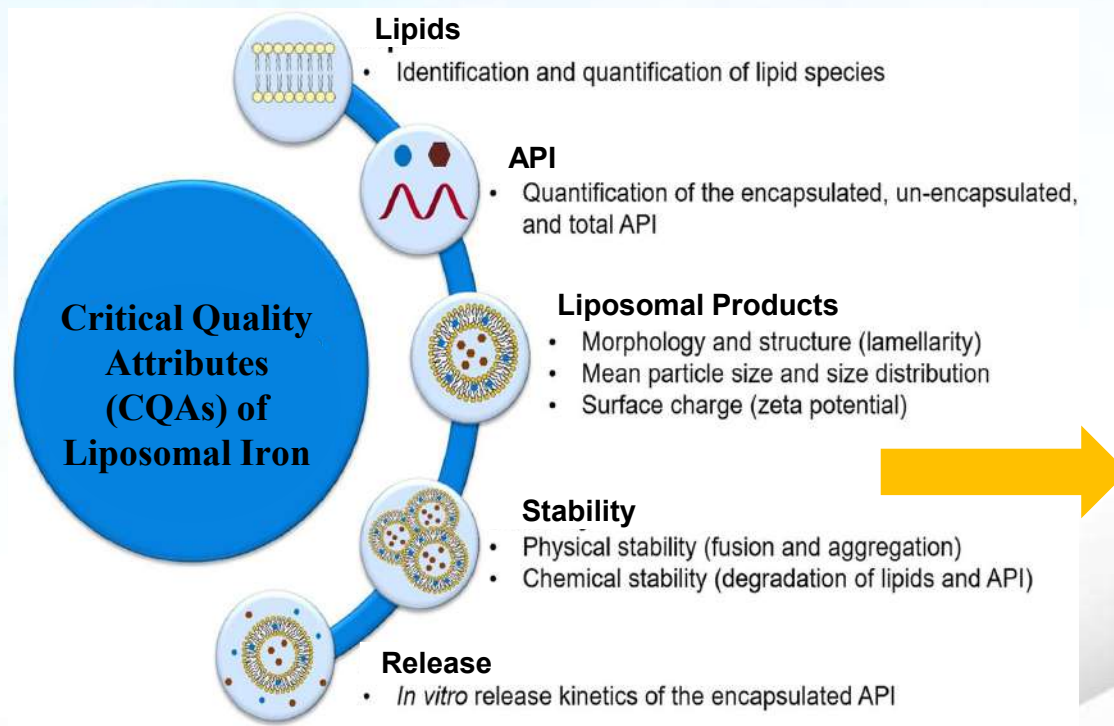
**Fe**

**LIPOSOMAL**

West Bengal Chemical Industries Limited

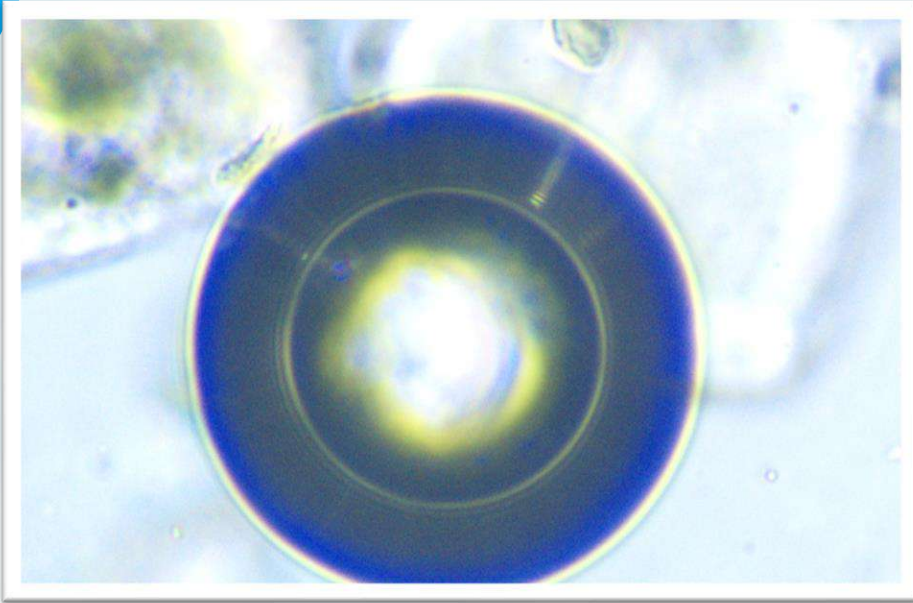


# Summary of Characterizations Performed on Liposomal Iron

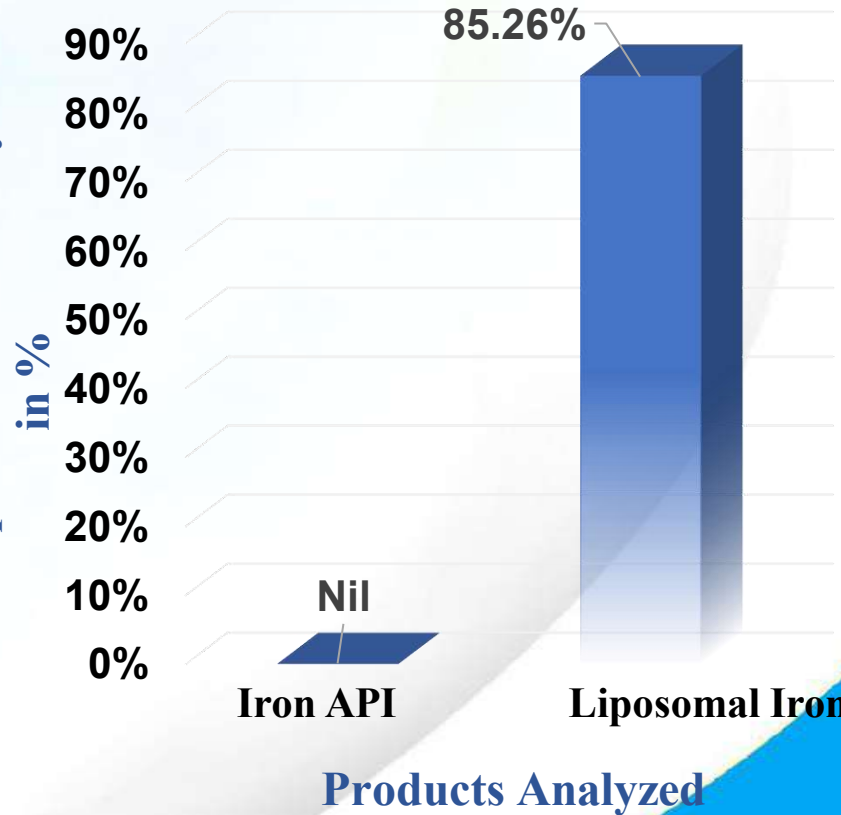


1. *Encapsulation efficiency of Liposomal Iron*
2. *Analysis of particle size and uniformity of Liposomal Iron using DLS*
3. *Behavior of Liposomal Iron particles in liquid medium using DLS Zeta-sizer*
4. *FTIR analysis of Liposomal Iron composition*
5. *Elemental analysis of Liposomal Iron*
6. *Morphology analysis of Liposomal Iron using SEM*
7. *Analysis of Iron leakage from Liposomes*
8. *Stability analysis of Liposomes at 105° C temperatures*
9. *Endothermic study of Liposomal Iron using DSC analysis*
10. *Thermogravimetric Analysis (TGA) of Liposomal Iron*
11. *Correlation between DSC & TGA*
12. *Mineral Loading Capacity*

# 1. Encapsulation Efficiency of 12% Liposomal Iron



Encapsulation Efficiency  
in %



## ❖ Acceptance criteria:

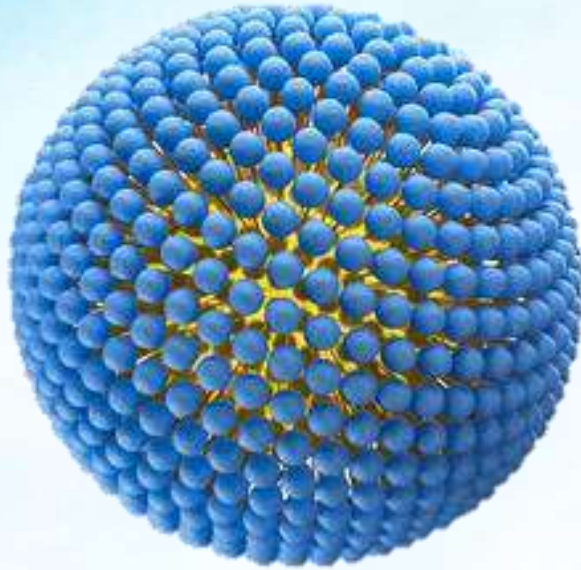
- Assay : **10% - 12%**
- Encapsulation efficiency : **NLT 70%**

Encapsulation Efficiency determined via validated titrimetric data

- Liposomal encapsulation ensures **85.26% efficiency**, significantly surpassing the **minimum requirement of 70%**.
- Efficient encapsulation minimizes **mineral loss**, improving **bioavailability** and **therapeutic efficacy**.
- Offers **protection against oxidation and gastrointestinal irritation**, common with conventional iron forms.



## 2. Dynamic Light Scattering Analysis of Liposomal Iron



**POLYDISPERSITY INDEX (PDI)**

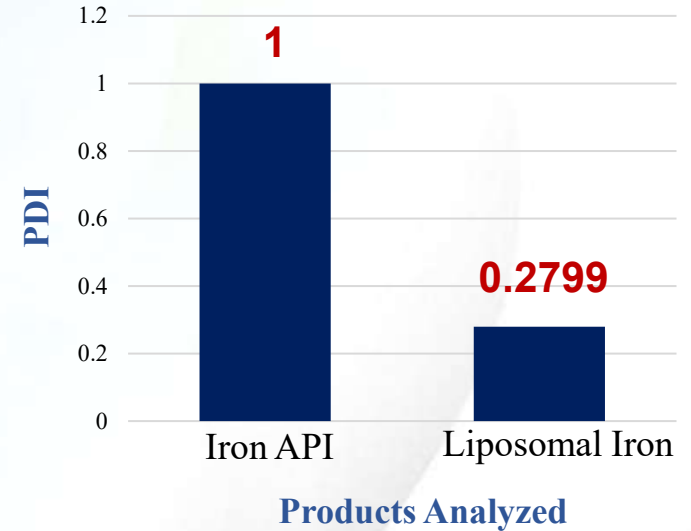


**Figure 1 – Polydispersity Index (PDI) of Liposomal Iron in solution**

- Liposomal Iron particles measure **~153.8 nm** compared to **~1942 nm** for raw Iron API, indicating nanoscale formulation.
- PDI reduced from **1.0** to **0.2799**, signifying a narrow particle size distribution.
- Nanosized, uniform particles offer greater colloidal stability and improved shelf life.
- Smaller particles support **increased mucosal permeability** and cellular uptake.
- **DLS characterization** confirms high formulation control and **batch-to-batch reproducibility**.

**PARTICLE SIZE**

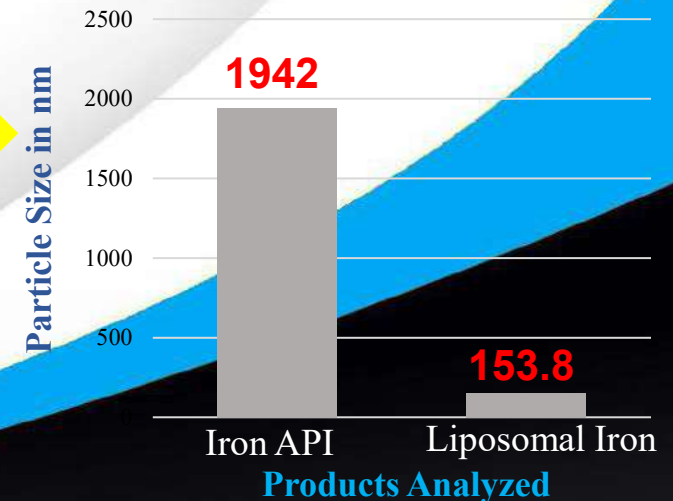


**Figure 2 – Chart showing the particle size of Iron API with Liposomal Iron**

# 3a. Behavior of Liposomal Iron

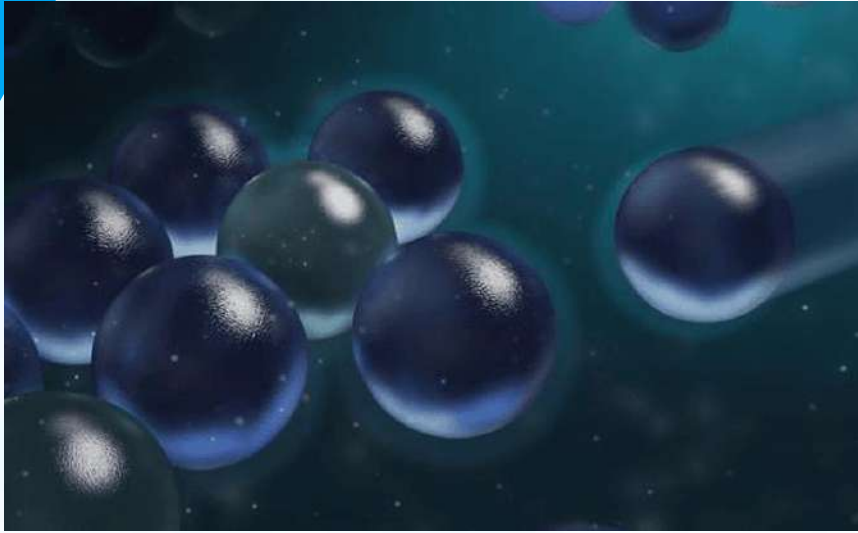


**Figure 1 – A figure showing the balance of attractive and repelling forces which determine how particles behave in a medium.**

- Liposomal Iron shows **high zeta potential (-61.22 mV)** → excellent colloidal stability.
- Prevents particle aggregation → ensures **uniform suspension**.
- Enhances **product shelf life** and **bioavailability** in liquid form.

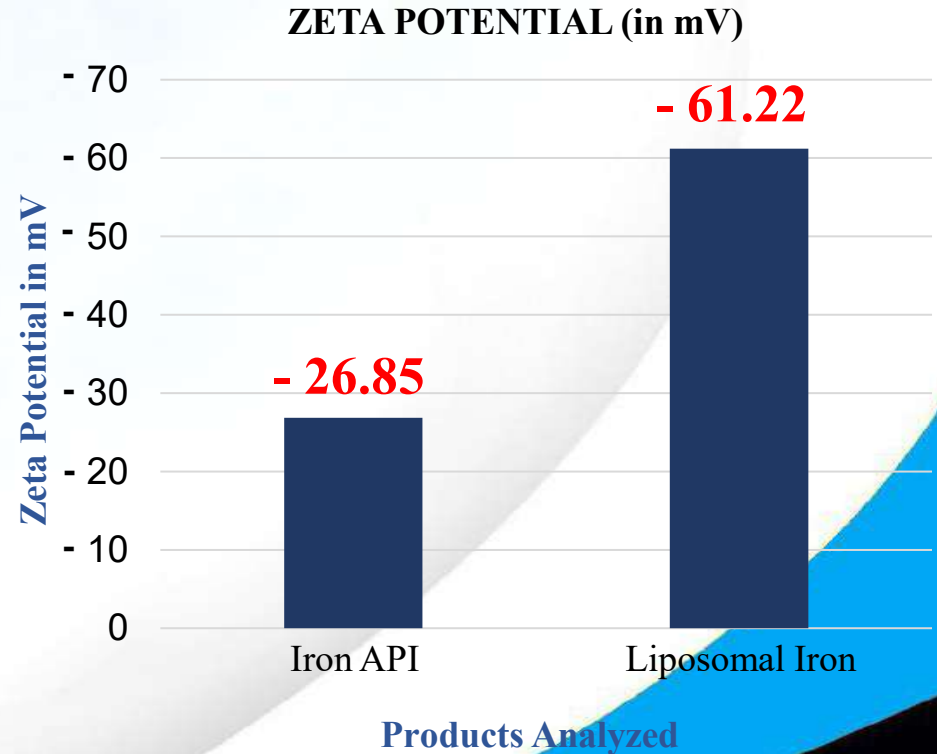


**Figure 2 – Chart comparing the zeta potential of Iron API and Liposomal Iron indicating that Iron in Liposomal form is stable and unlikely to agglomerate in solution.**

# 3b. Absorption of Liposomal Iron Represented Schematically on a Cellular Cross-Section

Mineral Release

Zeta Potential

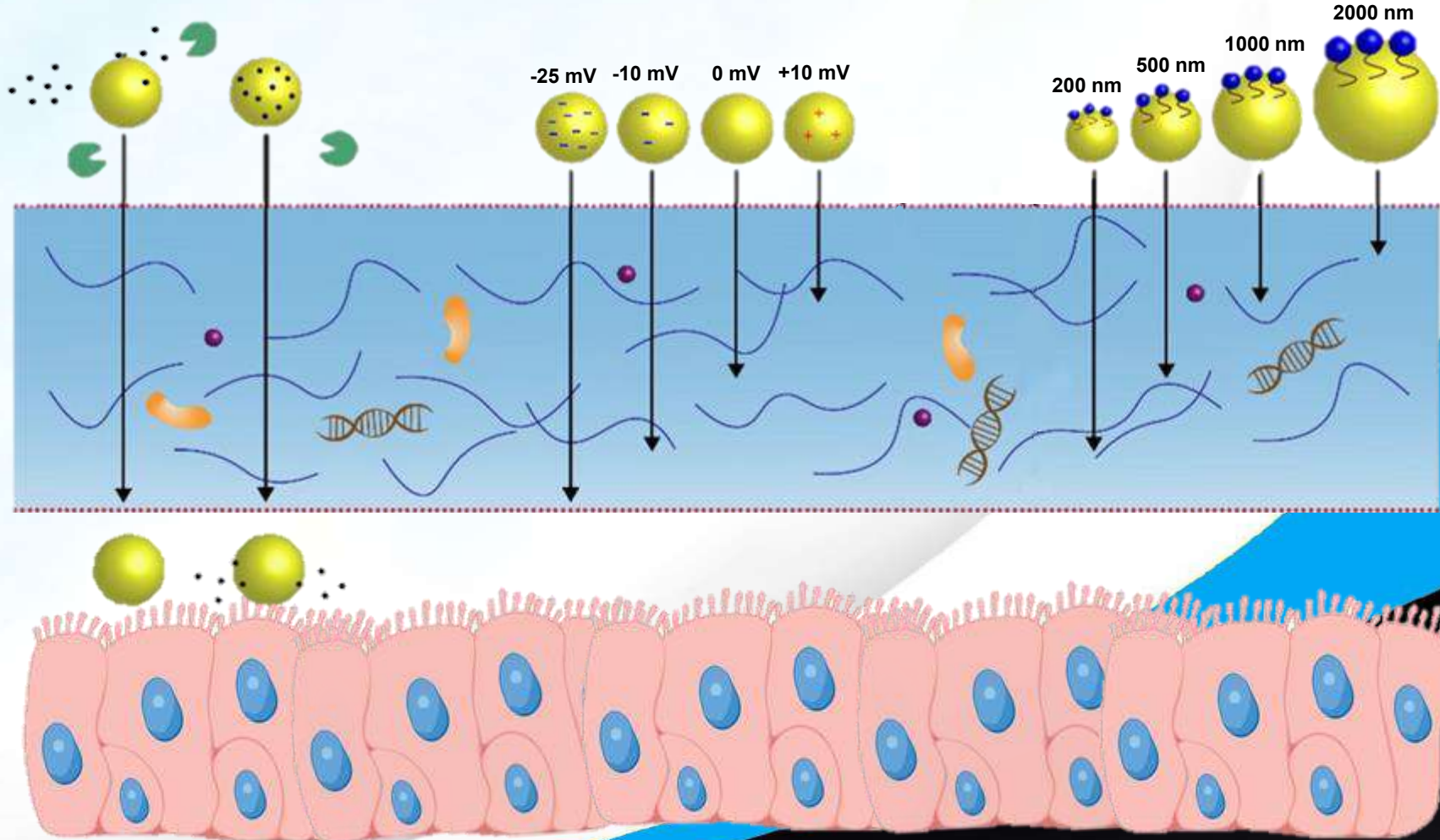
Particle Size

Lumen

Mucus Barrier

Absorption Membrane

Cellular Epithelium



Liposome

Mucus Permeation

Surfactant

Enzyme

Mucin

Lipid

Nucleic Acid

Protein

# 4a. FTIR Spectra of Iron, Liposome & Liposomal Iron

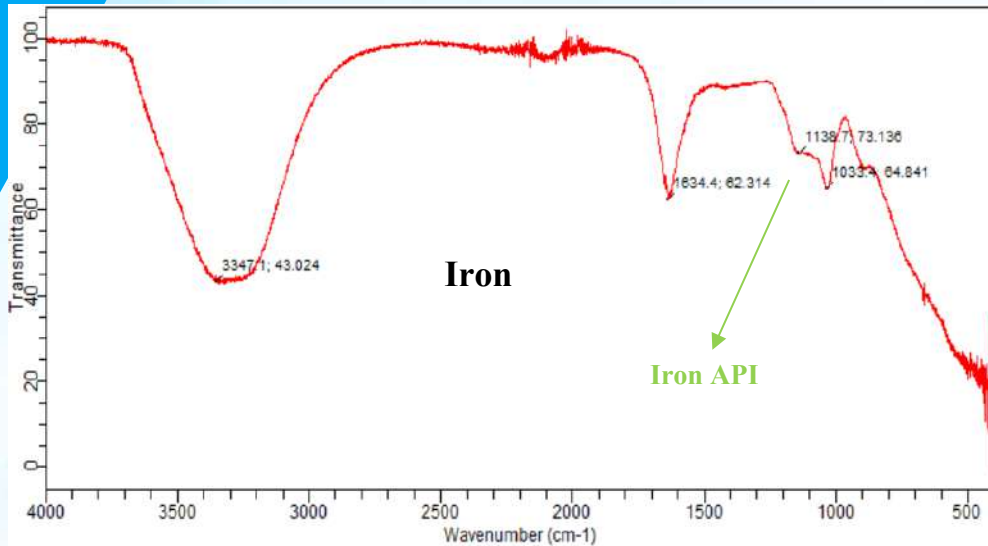


**Figure 1: IR Transmission spectrum showing characteristic bands of Iron API**

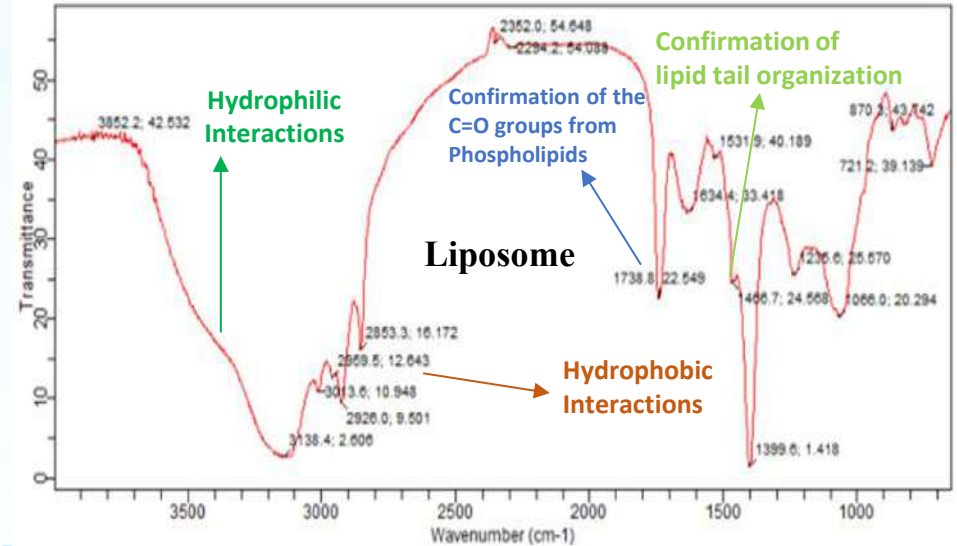


**Figure 2: Hydrophobic and Hydrophilic interactions within Empty Liposome**

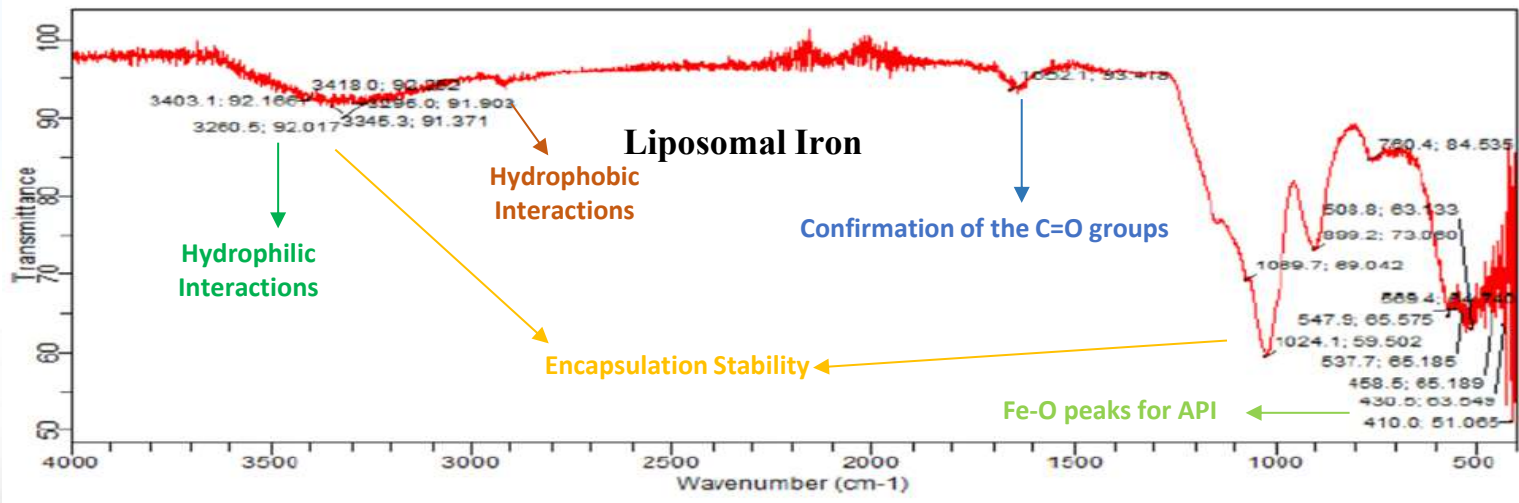


**Figure 3: Successful integration of Iron into Liposome**



## 4b. Summary of FTIR Analysis of Liposomal Iron

**1. Confirmation of the C=O and OH groups** - Peaks at  $1652.1 \text{ cm}^{-1}$  (C=O) and  $1024.1 \text{ cm}^{-1}$  ( $\text{PO}_4^-$ ) suggest strong interaction between ferric ions and lipids. Broad -OH peaks ( $\sim 3400 \text{ cm}^{-1}$ ) and shifts in C=O ( $1652.1 \text{ cm}^{-1}$ ) indicate sustained release due to hydrogen bonding.

**2. Hydrophobic Interactions** - Distinct  $\text{CH}_2$  stretching peaks at  $2920$  and  $2850 \text{ cm}^{-1}$  confirm ordered lipid tail packing.

**3. Hydrophilic Interactions** - Broad -OH peaks ( $\sim 3403.1, 3418.0 \text{ cm}^{-1}$ ) and  $\text{PO}_4^-$  stretching ( $1024.1 \text{ cm}^{-1}$ ) confirm strong interactions with ferric ions.

**4. API** - Fe-O peaks ( $\sim 410.0, 430.5 \text{ cm}^{-1}$ ) and  $\text{CH}_2$  stretching ( $\sim 2920, 2850 \text{ cm}^{-1}$ ) confirm the presence of ferric pyrophosphate within bilayer.

**5. Encapsulation Stability** - Stable, as indicated by  $\text{CH}_2$  stretching ( $\sim 2920, 2850 \text{ cm}^{-1}$ ) and Fe-O ( $\sim 410.0, 430.5 \text{ cm}^{-1}$ ).

# 5. Elemental Analysis of Liposomal Iron

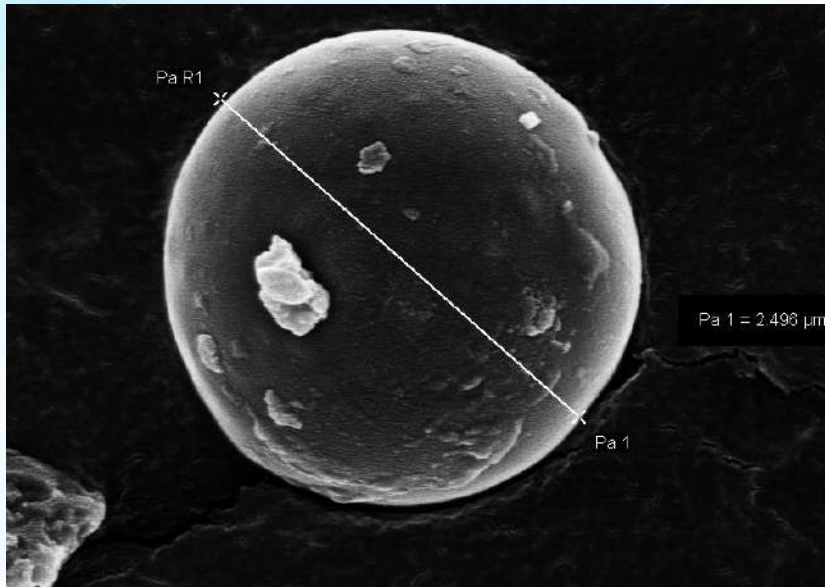
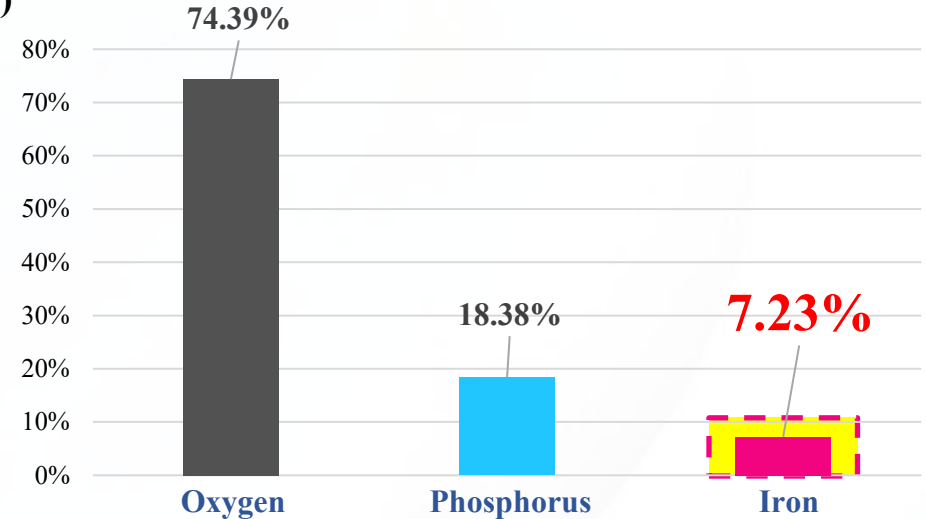


**Figure 1 – SEM imaging showing the area scanned using Energy Dispersive X-Ray Spectroscopy (EDAX)**

**(a) ELEMENTAL COMPOSITION OF IRON API**



**(b) ELEMENTAL COMPOSITION OF LIPOSOMAL IRON**

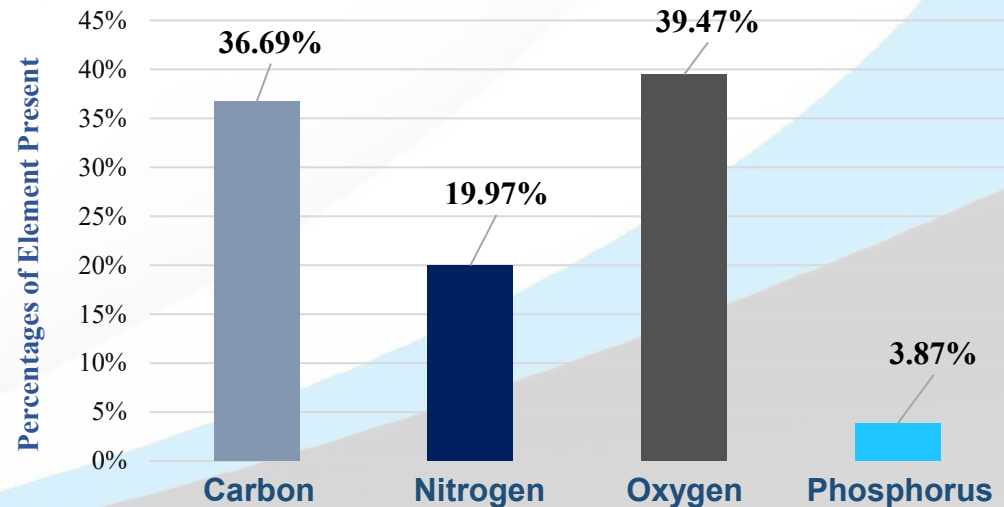


**Figure 2 – A graphical representation of the percentages of elements composing (a) Iron API and (b) Liposomal Iron**

- **Iron API contains Oxygen (74.39%), Iron (7.23%) and Phosphorus (18.38%)** as major elements, with moderate Carbon, Oxygen, and Nitrogen levels.
- **Liposomal Iron shows no detectable Iron on the surface**, indicating successful encapsulation and formulation change.
- **Carbon (36.69%) and Oxygen (39.47%) dominate** in the Liposomal form, with reduced Phosphorus (3.87%).

# 6. Morphology of Liposomal Iron as Viewed Under Scanning Electron Microscope

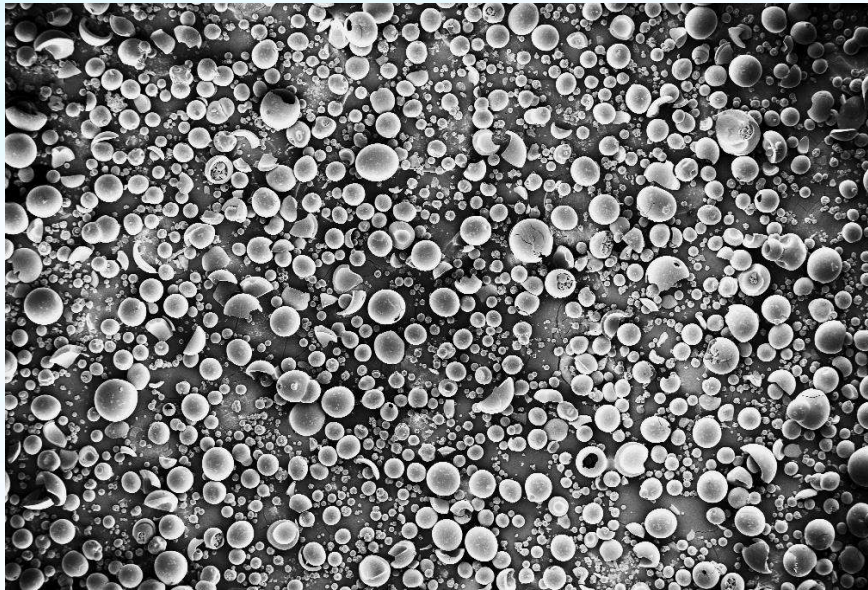


**Figure 1 – SEM image of few scattered Iron Liposomes scattered within the field of view under observation**

- Spherical morphology observed in Liposomal iron particles.
- Uniform size distribution seen across the field (Figure 1).
- Particles appear smooth-surfaced at low magnification.
- Spherical and uniform morphology enhances **stability, encapsulation efficiency, and cellular uptake**, making it ideal for Liposomal drug delivery.

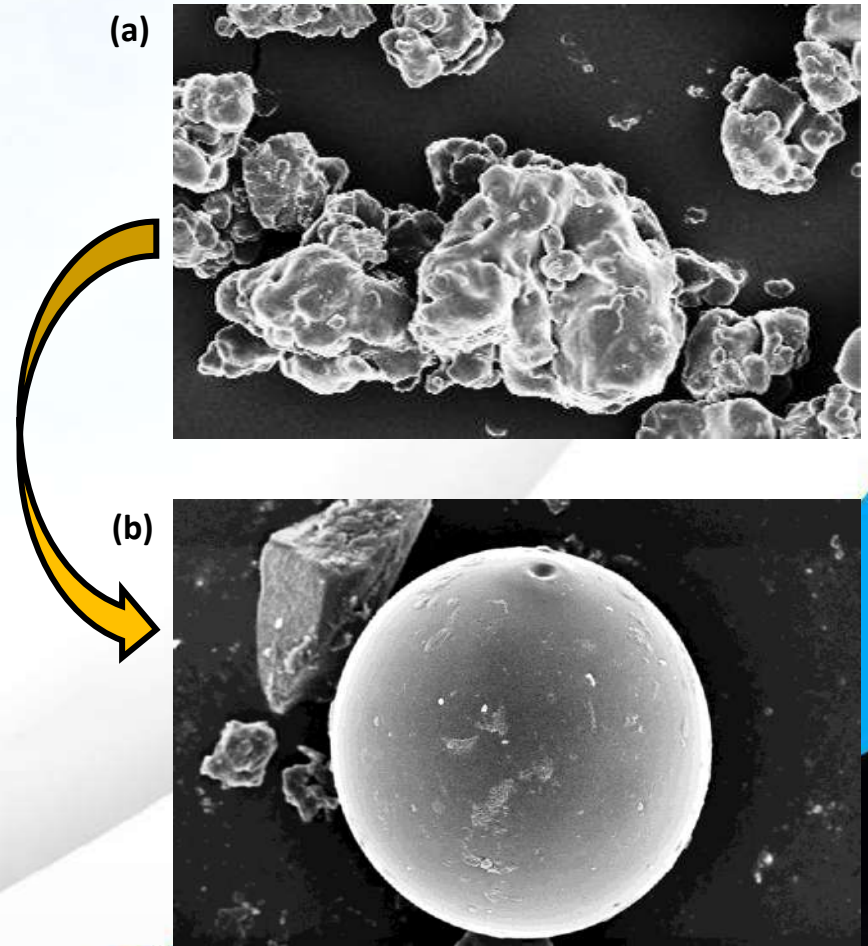


**Figure 2 – SEM panels showing transformation from (a) Iron API to (b) Liposomal Iron after encapsulation.**

# 7. Leakage of Liposomal Iron



Figure 1 – An image representing the storage of formulations in shelves

- Iron leakage is very low over 3 years under accelerated stability conditions.
- Product stability is maintained as encapsulation efficiency stays above the acceptance criterion of NLT 70%.

% of Iron & Encapsulation Efficiency

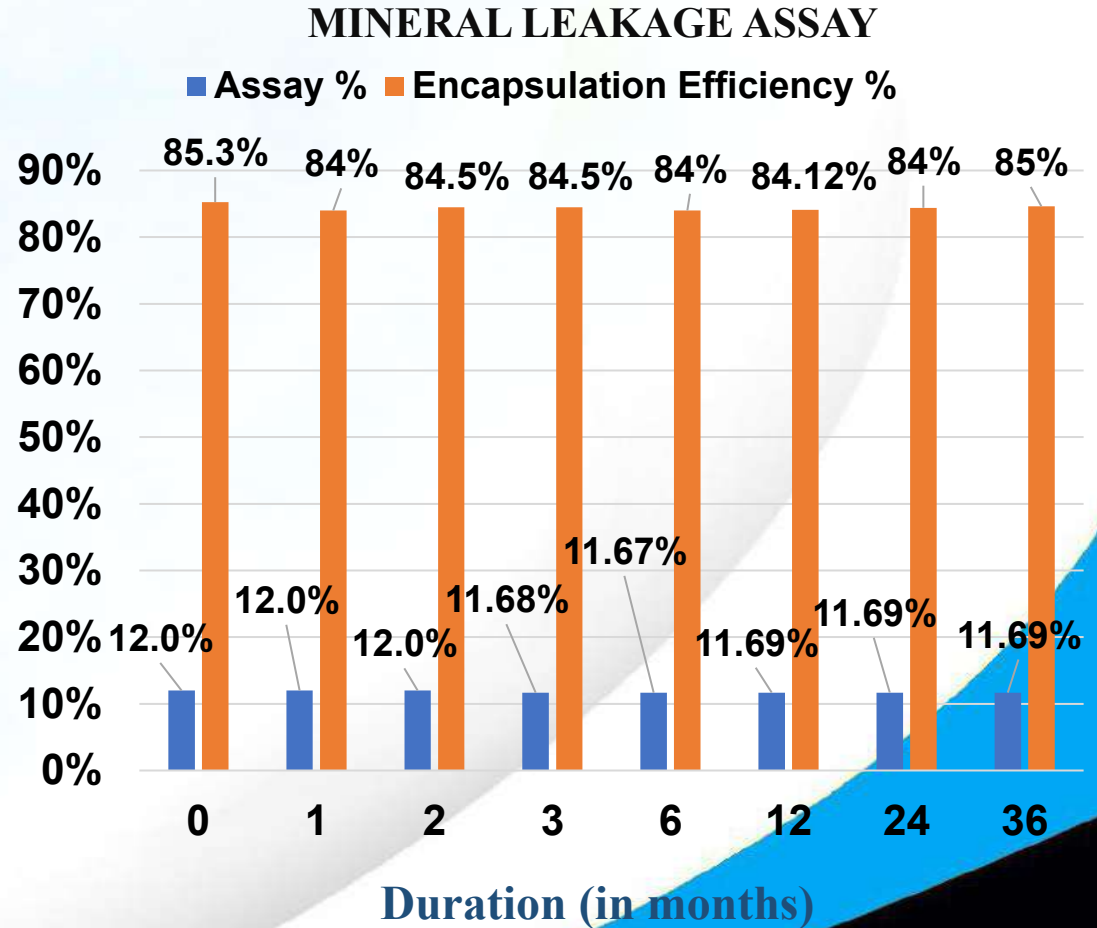


Figure 2 – Chart comparing the stability of Liposomal Iron stored over a period of 3 years at 40°C ± 2°C and a relative humidity of 75% ± 5%.

# 8. Stability of Liposomal Iron at Elevated Temperatures

## TEMPERATURE EXPOSURE STUDY



Figure 1 – Illustration depicting the transport of formulations at elevated temperature.

- Encapsulation efficiency remains high ( $\approx 85\%$ ) even after exposure to  $105^\circ\text{C}$  for 4 hours.
- Assay values ( $12\%$  at RT vs.  $11.68\%$  at  $105^\circ\text{C}$ ) show minimal variation, indicating negligible iron leakage.
- Demonstrates **thermal robustness**, making the formulation suitable for transport and storage in hot climates.

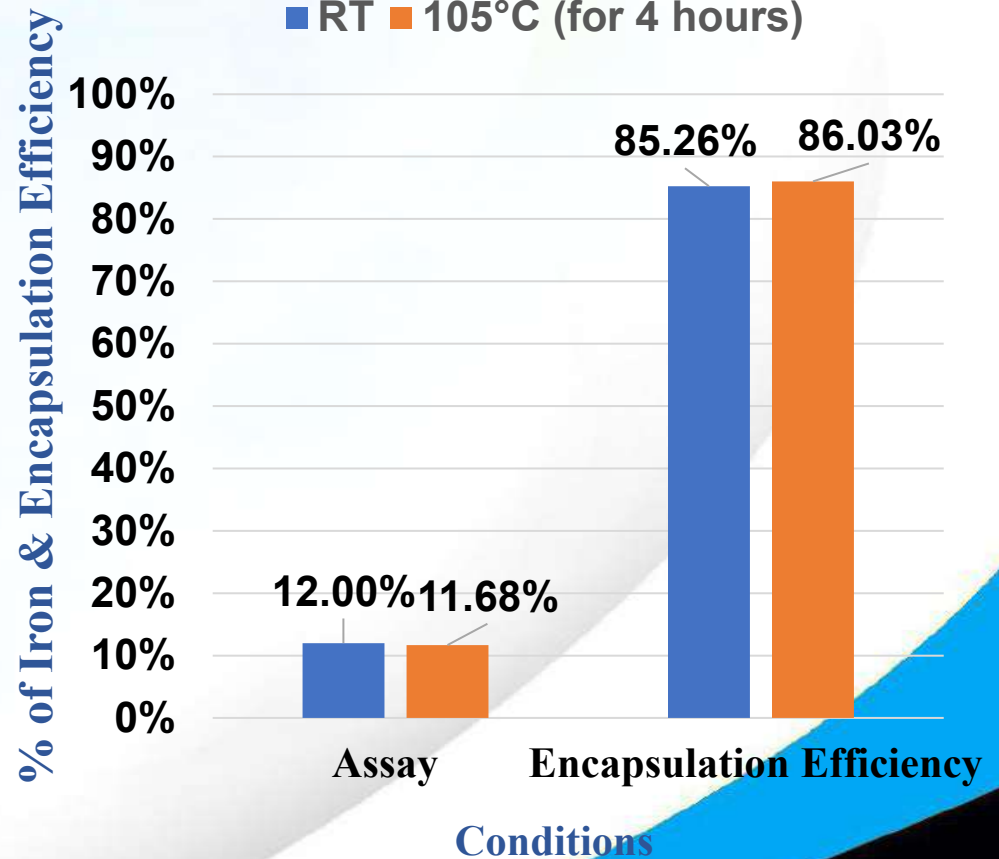


Figure 2 – Chart comparing the stability of Liposomal Iron both at room temperature (RT) and at  $105^\circ\text{C}$  for 4 hours of exposure.

# 9a. Differential Scanning Calorimetry Analysis

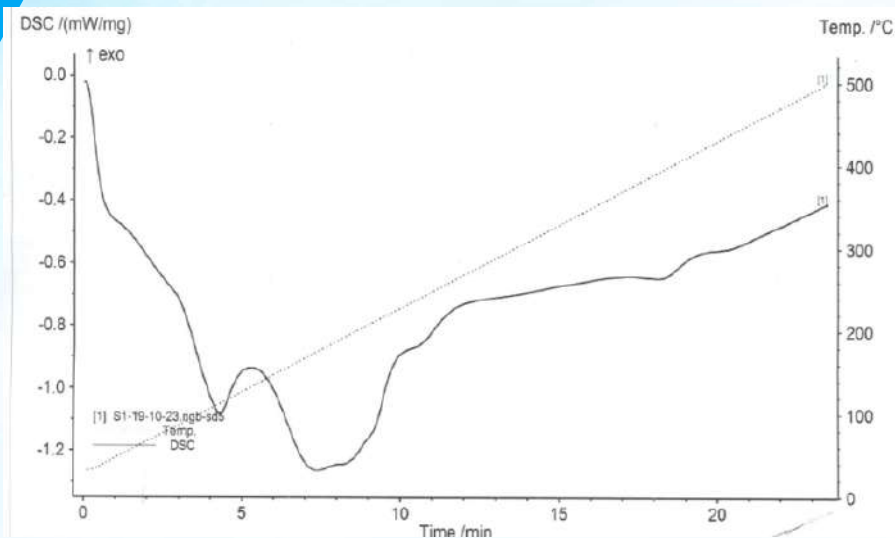


Figure 1: DSC Thermogram of Iron API

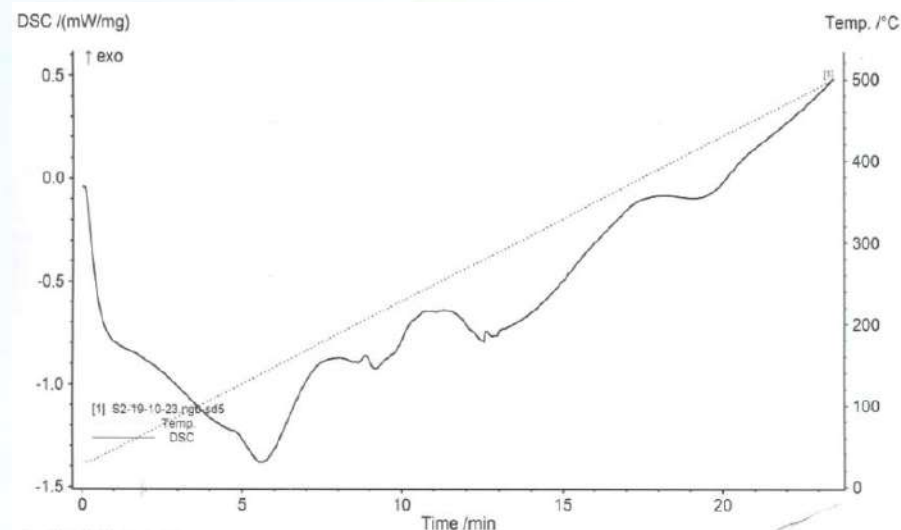


Figure 2: DSC Thermogram of Empty Liposome

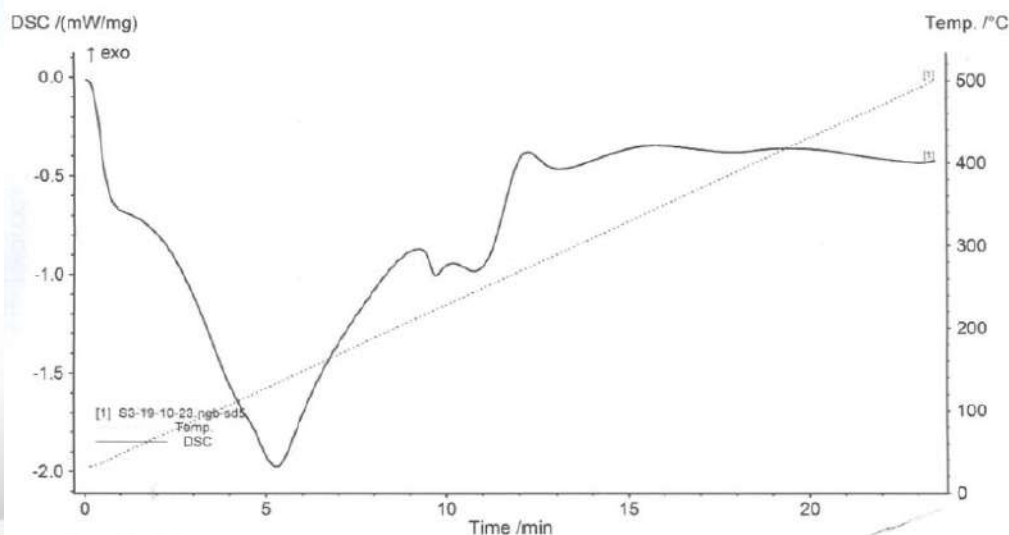
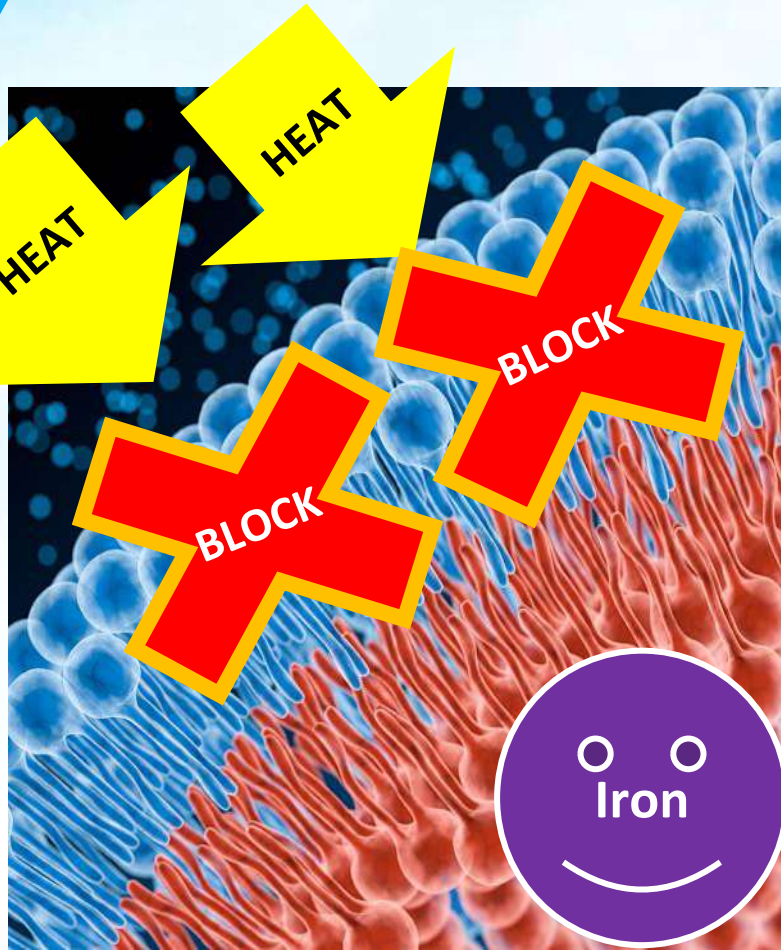


Figure 3: DSC Thermogram of Liposomal Iron

# 9b. Endothermic Study of Liposomal Iron Using Differential Scanning Calorimetry Analysis



An illustration showing how the phospholipid bilayer is hindering the heat from reaching Iron API which improves thermal stability of Liposomal Iron.

Sample	Thermal Events (°C)	Inference
<b>Iron API</b>	112.23, 177.67	Distinct thermal transitions indicate phase changes or melting points associated with ferric pyrophosphate*.
<b>Liposome</b>	136.85, 212.78, 278.42	Exhibits multiple transitions related to phospholipid structural changes and thermal stability*.
<b>Liposomal Iron</b>	132.30, 223.04, 288.63	Reduced enthalpy changes indicate successful encapsulation and stabilization within the lipid matrix. Higher thermal stability reflects strong bonding between lipid bilayer and ferric pyrophosphate*.

# 10. Thermogravimetric Analysis of Liposomal Iron

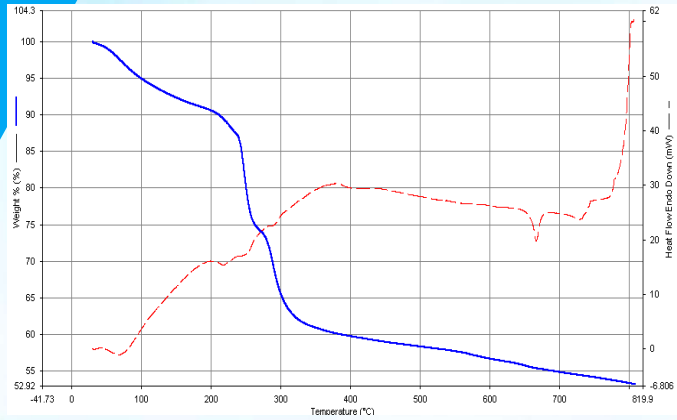


**Figure 1 – A Thermogravimetric Analysis (TGA —) and Differential Thermogravimetric Analysis (DTA ---) plots showing structural changes summarized as follows:-**

- TGA: ~7.6% loss (30–150 °C) → ~11.8% (150–250 °C); major structural/condensation change with ~19.7% loss (250–350 °C). Residue at ~809 °C ≈ 53%.
- DTA (Endo ↓): broad low-T endotherm for moisture; ~217 °C; high-T endotherms (~667/728/753 °C) then strong exotherm (~805 °C).

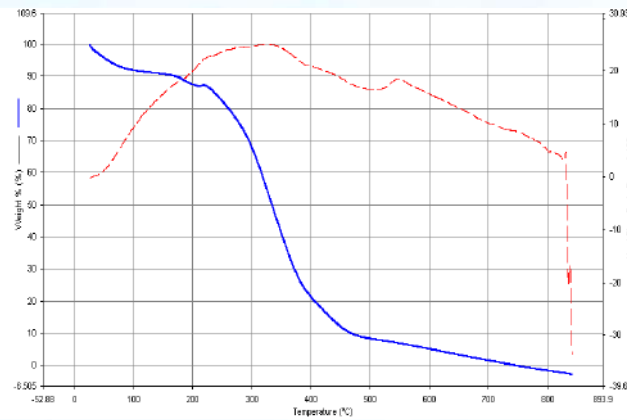


**Figure 2 – A Thermogravimetric Analysis (TGA —) and Differential Thermogravimetric Analysis (DTA ---) plots showing structural changes summarized as follows:-**

- TGA: ~9% mass loss from ~26 → ~139 °C (free → bound water/volatiles); no discrete decomposition step.
- DTA (Endo ↓): broad 40–90 °C endothermic drift without sharp peaks (dehydration signature).

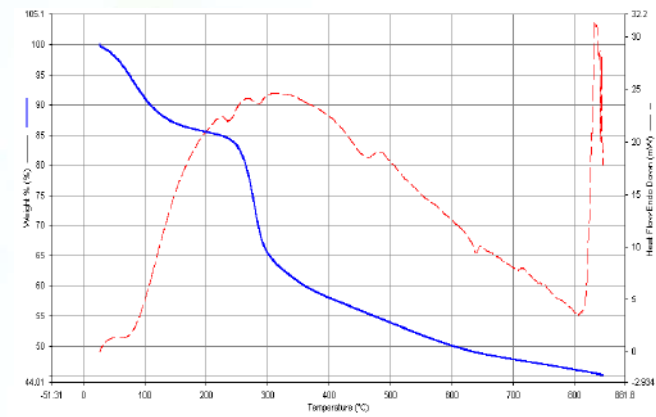


**Figure 3 – Here mass loss analysis from (TGA —) and (DTA ---) plots showing structural changes summarized as follows:-**

- TGA: continuous ~12–13% mass loss from ~27 → ~138 °C, steeper over 50–100 °C (moisture from lipid matrix + associated/entrapped water).
- DTA (Endo ↓): broad endothermic baseline shift through ~40–130 °C, no sharp transitions—consistent with dehydration, not melting/reaction.



# 11. Correlating DSC and TGA of Liposomal Iron

Parameter	Analysis purpose	Analogy
DSC (Differential Scanning Calorimetry)	Measuring how much heat a material absorbs or releases as it's heated	Burning a log and seeing how much ash is left.
TGA (Thermogravimetric Analysis)	Checking if the material is losing weight as it's heated — from things like evaporation or breakdown.	Melting chocolate and measuring how much heat is needed.



## Why Correlation Matters:

If both DSC and TGA respond at the same temperature, it means a real change is happening — both inside the material (DSC) and on the outside (TGA).

The material is **physically changing** (e.g., losing water or breaking down)

And it's also **thermally active** (taking in or releasing energy)

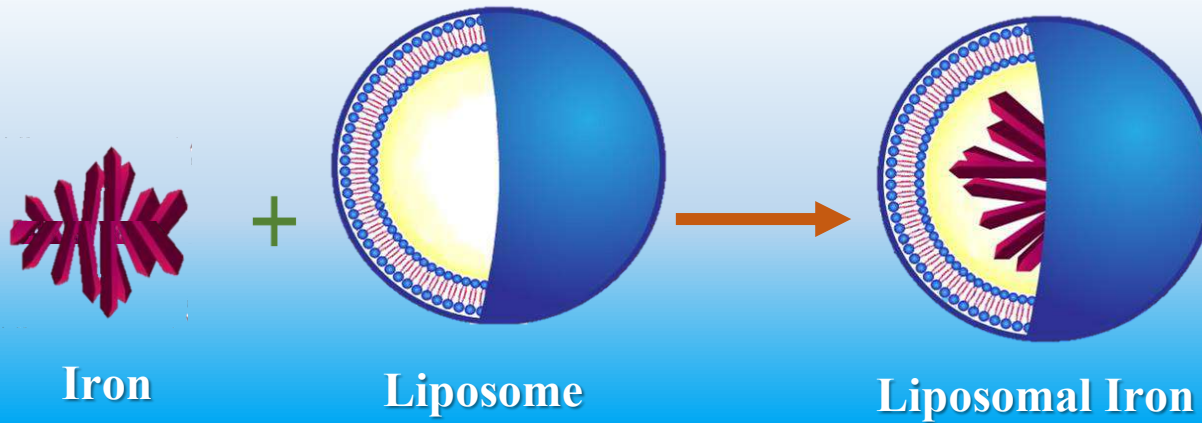
## Correlation Summary

Temp (°C)	DSC Obs.	TGA Obs.	Correlation	
112.23	Clear	No loss	◇ Phase transition (Iron)	Iron API
177.67	Yes	~0.1%	◆ Structural rearrangement	
800	Yes	~54% residual	✓ Stable iron oxide	
136.85	Yes	~15% (~200-300°C)	◆ Main lipid decomposition	Empty Liposome
212.78	Yes	Minor change	✓ Initial degradation	
278.42	Yes	~70% (~500°C)	✓ Final decomposition	
841	Yes	~1.58% residual	✓ Minimal impurities	Liposomal Iron
223.04	Yes	~13.7% (~150°C)	✓ Multi-stage decomposition	
288.63	Yes	~37% (~400°C)	✓ Enhanced stability	
800	Yes	~45% residual	✓ Stable iron oxide	

# 12. Mineral Loading Capacity

**Iron Loading**

**0.71 mg per mg of Liposomal Product**



Formulation of Iron in Liposomes

- Iron loading capacity in Liposomes refer to the amount of Iron encapsulated within the Liposome relative to the total weight of the Liposomal formulation.
- A higher Iron loading capacity in Liposome ensures more efficient mineral delivery, reduces the amount of Liposome required, and improves therapeutic outcomes.

$$\text{Iron loading capacity} = \frac{\text{Mass of Iron in Liposomal Iron}}{\text{Total mass of Iron and Liposome}}$$

# Thank You!

**WEST BENGAL CHEMICAL INDUSTRIES LIMITED**

*(A Joint Venture with Government of West Bengal | A cGMP & ISO 9001 : 2015 Certified Company)*

145/1, Jessore Road, Lake Town, Kolkata - 700 089, India.



[wbcil@wbcil.com](mailto:wbcil@wbcil.com)



[www.wbcil.com](http://www.wbcil.com)



+91 (033) 4025 1555 / 1539

